Chinese Journal of Physiology 60(1): 41-53, 2017
DOI: 10.4077/CJP.2017.BAF449

Double Labeling of Vagal Preganglionic and Sympathetic Postganglionic Fibers in Celiac Ganglion, Superior Mesenteric Arteries and Myenteric Plexus

Shi-Jane Ting[1], Chih-Kuan Kao[1], and Feng-Bin Wang[1, 2, 3, 4]

[1]*Department of Psychology, National Chung Cheng University, Chiayi 62102*
[2]*Mental Health Promotion Center, National Chung Cheng University, Chiayi 62102*
[3]*Doctoral Program in Cognitive Sciences, National Chung Cheng University, Chiayi 62102*
and
[4]*Advanced Institute of Manufacturing with High-Tech Innovations, National Chung Cheng University, Chiayi 62102, Taiwan, Republic of China*

Abstract

Sympathetic efferents regulate the "fight-or-flight" response and sympathetic and vagal fibers have been suggested to retrogradely and centrally spread pathogens associated with Parkinson's disease. To examine the arrangement of the vagal and sympathetic motor fibers in the celiac ganglion (CG), gastrointestinal (GI) tract, and along the superior mesenteric artery (SMA) and its sub-branches, we double-labeled the vagal efferents by injecting Dextran-Texas Red into the dorsal motor nucleus of the vagus and the sympathetic postganglionics with tyrosine hydroxylase (TH) immunohistochemistry in male Sprague-Dawley rats (n = 18). The laser scanning confocal microscope was used for image analysis. Vagal nerve endings were densely distributed around the CG neurons, and the right CG received more. Vagal and sympathetic efferent endings formed various ring or string shapes that tangled closely in the myenteric plexus of the forestomach, duodenum, jejunum and ileum. Vagal and sympathetic efferents coursed within the same nerve bundles before reaching the myenteric plexus, had in-apposition varicosities, and ran parallel with the SMA and its sub-branches. Although a complete sympathetic tracing and an incomplete tracing and/or damage to the vagal preganglionic neurons may lead to a sampling bias, the sympathetic innervations in the blood vessels and myenteric plexus are stronger than in the vagus. The in-apposition innervation varicosities of the vagal and sympathetic efferents within the same nerve bundles and in the myenteric plexus of the gut with complex innervation patterns may offer a network to automatically control GI functions and an infection route of the Parkinson's disease between the autonomic efferent endings.

Key Words: autonomic, Dextran-Texas Red, myenteric plexus, parasympathetic, sympathetic, tyrosine hydroxylase immunohistochemistry

Introduction

The motor outflow of the autonomic nervous system consists of two divisions: the sympathetic and parasympathetic nervous systems. Both are organized hierarchically into pre- and postganglionic levels, and the sympathetic division has much more rapid and strong regulation in the "fight-or-flight" response than does the parasympathetic (5, 21). We have previously characterized two types of vagal afferents in the muscle of the gastrointestinal (GI) tract from oral esophagus to the colon presumably with different functions: intraganglionic laminar endings (IGLEs) are to integrate intramural tension, and intramuscular arrays (IMAs)

Corresponding author: Dr. Feng-Bin Wang, Department of Psychology, National Chung Cheng University, Chiayi 62102, Taiwan, R.O.C. Tel: +886-5-272-0411 ext. 32208, E-mail: psyfbw@ccu.edu.tw
Received: June 10, 2016; Revised (Final Version): August 11, 2016; Accepted: August 23, 2016.
 ISSN : 0304-4920. http://www.cps.org.tw

appear to work as stretch receptors (22, 24). This inventory leads to further examination of the hypothesis that IMAs may operate as stretch detectors (15, 16, 18). Similarly, an inventory of the vagal and sympathetic efferents may offer insight to further understand the motor regulation of the gut. Moreover, we have documented that vagal afferents always deliver two nerve bundles running along each branch of the superior mesenteric artery (SMA) (23); we wondered how the sympathetic and vagal efferents were arranged in the vasculatures of the GI tract.

The parasympathetic and sympathetic pre- and postganglionic neurons are involved in the development of the Parkinson's disease (3, 4, 6). The diagnostic features of Parkinson's disease, the alpha-synuclein-positive Lewy bodies and Lewy neurites, first occur in the autonomic pathways in the GI tract during the earliest and pre-symptomatic stage of the disease (4). Hypothetically, an environmental pathogen of Parkinson's disease may first breach the mucosal barrier of the GI tract in susceptible individuals, infect α-synuclein-positive neurons in the enteric nervous system, and subsequently the vagal preganglionic fibers spread the pathogen to the central nervous system (9). The GI tract is heavily innervated by vagal preganglionics (1, 8). Thus, Hawkes *et al.* (9) suggested that the stomach is the most likely starting point for any pathological insult to reach the dorsal vagal complex. The expression of α-synuclein in the myenteric neurons increases proportionally from the stomach through duodenum to jejunum (14). Furthermore, all vagal preganglionic projections, but not vagal afferent endings, express α-synuclein both in axons and terminal varicosities that being in apposition with the myenteric neurons (14).

In Braak's infection model of the Parkinson's disease (4), the celiac ganglia (CGs) are the sites that the sympathetic postganglionic neurons send axons to the enteric nervous system to contact the vagal preganglionic elements as the infection route. As demonstrated by Berthoud and Powley (2), the vagal efferent fibers were found to penetrate widely into the prevertebral ganglia, including the CGs, superior mesenteric ganglion, some of the associated microganglia, and suprarenal ganglia. Vagal efferents formed varicose terminal-like structures that suggest synaptic contacts to individual ganglion cells. However, double labeling of the vagal preganglionic and sympathetic postganglionic efferents at the visceral terminal ends has nerve been reported.

Although the abdominal vagal nerves contain small amount of catecholaminergic fibers coming from neurons in the dorsal motor nucleus of the vagus (dmnX) and nodose ganglia (19, 25), Dextran-Texas Red and tyrosine hydroxylase (TH) have been well established to respectively trace the vagal preganglionic (17, 20) and sympathetic postganglionic efferents (7, 10-12). To examine the general arrangement of the vagal and sympathetic motor fibers innervating the CG, GI tract and mesenteric arteries, we double labeled the vagal efferents by injecting Dextran-Texas Red into the dmnX and the sympathetic postganglionics by TH immunohistochemistry in the rats.

Materials and Methods

Subject Housing Environment

Male Sprague-Dawley rats (n = 18; 3-5 months old, 280~350 *g*), obtained from BioLASCO (Taipei, Taiwan), were housed individually and maintained on a 12-h light/dark cycle at room temperature 23–25°C. Solid food chow and tap water were available *ad libitum*. All experimental treatments were under the guidelines of the Council of Agriculture, Executive Yuan, ROC, and approved by the Institutional Animal Care and Use Committee of National Chung Cheng University.

Labeling of Vagal Preganglionic Efferents

After overnight food deprivation, rats were anesthetized with sodium pentobarbital (50-55 mg/kg, ip). To label selectively the vagal efferent innervation in the CG, SMA, and myenteric plexus of the forestomach and small intestines, from the duodenum to the ileum, the red fluorescent dye Dextran-Texas Red (5%; 10,000 MW, lysine fixable; D-1863; Molecular Probes, Eugene, OR, USA) was pressure injected (0.5–0.6 μl total volume, five sites on each side: two rostral to, one at, and two caudal to the area postrema) *via* glass micropipettes bilaterally into the dmnX with Picospritzer II, (50 lbs pressure, 4~6 msec/pulse). The wound was closed and treated with antibiotic powder (Neomycin sulfate). After recovering on a heating pad (36°C), the animal was returned to its home cage. The rats were maintained for 19 days post-injection to allow the transport of the dye (17).

Fluorescent Immunohistochemistry for TH

Rats were injected with a lethal dose of sodium pentobarbital (180 mg/kg, ip) and perfused through the left ventricle of the heart with 200 ml 10 mM sodium phosphate buffer saline (PBS; pH 7.4; 38°C), followed by 500 ml 4% paraformaldehyde in 0.1M PBS (pH 7.4; 4°C). The CGs were reserved and sectioned into a thickness of 60 μm with a microtome. Tissue blocks reserved *en bloc* for examination included the forestomach, duodenum (the first 4 cm of the small intestine distal to the pyloric sphincter), jejunum (four 1-cm whole mounts randomly sampled approximately 52 cm distal to the pyloric sphincter) and ileum (the last 3 cm of the small intestine rostral to the cecum),

and the SMA with finer sub-branches. The stomach was filled with 5 ml water before perfusion to ensure a standard size with an appropriate muscle thickness. The whole mounts of the dorsal and ventral stomach were divided by cutting along the greater and lesser curvatures. The duodenum, jejunum and ileum were opened with a longitudinal cut along the mesenteric attachment. The block of vessels and mesentery was trimmed from the duodenum, jejunum and ileum just at the intestinal mesenteric attachment. If necessary, the vessels and hollow organs were flushed and cleaned with saline or water. Whole mounts were fixed for additional 2 h in 4% paraformaldehyde (in 0.1 M PBS). For penetration of the primary antibodies to the myenteric plexus, fat tissue, the mucosa and submucosa were peeled off with pairs of no. 7 forceps.

Whole mounts were rinsed in PBS and then soaked for 5-6 days at room temperature in PBS containing 5% normal goat serum, 2% bovine serum albumin, 0.5% Triton X-100, and 0.08% Na azide, followed by incubation for 24 h at room temperature in a rabbit primary antibody diluted with PBS containing 2% normal goat serum, 2% bovine serum albumin, 0.3% Triton X-100, and 0.08% Na azide. The primary antibody used was rabbit anti-phospho-TH (Ser19) (1:1000; 381402A; CA, USA). Whole mounts were then rinsed for 6 min 5 times in PBS and 0.3% Triton X-100 (PBST), and incubated for 2 h at room temperature in a solution consisting of goat anti-rabbit ALEXA Fluro 488 (1:500; A11034; Molecular Probes) diluted with PBST. Finally, labeled whole mounts were rinsed for 6 min 5 times in PBS, mounted on gelatin-coated slides, air-dried overnight, dehydrated in alcohol, and cleared in Xylene.

Confocal Microscopy and Image Processing

Confocal images were obtained using the Zeiss LSM510 confocal microscope (Carl Zeiss, Inc, Jena, Germany) that was controlled by the Zeiss LSM digital microscopy software. Double-labeled sections were imaged by using filter sets appropriate for the specific visualization of Texas Red (DSU-MRFPHQ) and ALEXA Fluor 488 (U-MNIBA2). Objective lens with 20x, 40x and 63x (oil-immersion; n.a. = 1.0, 1.0 and 1.4, respectively) were used.

Continuous images of the tissues sampled were created by z-series optical sections with adequate z-increments. Images were captured, analyzed and post-processed using the LSM Image Browsers Rel. 4.2 software. In some cases, z-stacks were compressed into one focus plane, *i.e.* maximum value projection. To test for apposition, single sections at the same focus plane were taken out of the z-stacks and the two channels were merged.

We used 20x objective lens for quick scan of the nerves and higher power lens (40x, 63x) for details. To determine the type of the vagal and sympathetic efferent nerve endings, the images were scanned randomly from different areas, the types of nerve endings were classified based on their shape, the frequency of each type was obtained, and the 3-D panels were transformed into 2-D for presentation.

Final post-production was done using the LSM Image Browsers Rel. 4.2 software and Photoshop CS2 software (Adobe Systems, Mountain View, CA, USA) to: (1) apply text and scale bars; (2) make minor adjustments to the color, brightness, contrast and sharpness of the images to match as closely as possible the appearance of the original material viewed under the microscope; (3) remove artifact (*i.e.* dust and lint), and (4) to organize the final layout of the figures.

Quantitative Analysis

The density of the vagal efferents and sympathetic postganglionic fibers, labeled respectively with Texas Red and ALEXA Fluor 488, in the myenteric plexuses of the forestomach, duodenum, jejunum and ileum was determined by counting the numbers of intersection points created by the fibers crossing with the horizontal and vertical grid lines (Fig. 1E). The grid was a square with 16x16 lines to fit in the square figures sampled from different magnification with different length: 428.5 μm (20x), 230.3 μm (40x), and 146.2 μm (63x) as shown in Fig. 1E (22).

Sequential optical sections of the autonomic fibers were scanned and the brightest section was sampled for area measurement. Areas of the vagal and sympathetic efferents distributed in the SMA and myenteric plexuses of the forestomach and small intestines were estimated by contouring the outer edges of the autonomic fibers scanned with 40x and 63x objective lens (Fig. 1F). The areas of the vagal (V) or sympathetic (S), or the areas with both autonomic efferents (vagal and sympathetic efferents in apposition) distributed in close apposition (A) were separately measured. The area percentages were calculated as (V, S, or A)/(V+S+A) × 100%. The area sizes sampled from the tissue were 230.3 × 230.3 μm^2 and 146.2 × 146.2 μm^2 respectively for 40x and 63x objective lenses. All quantitative data were analyzed with two-way analysis of variance (ANOVA) by SPSS.

Results

The continuous images from circular muscle to longitudinal muscle were created by z-series of up to 32 optical sections for the forestomach and 18 sections for the small intestines at z-increments of 1.5 μm for the forestomach and 0.8 μm for the small intestines (Fig. 1). As shown in Fig. 1G, the area of in-apposition

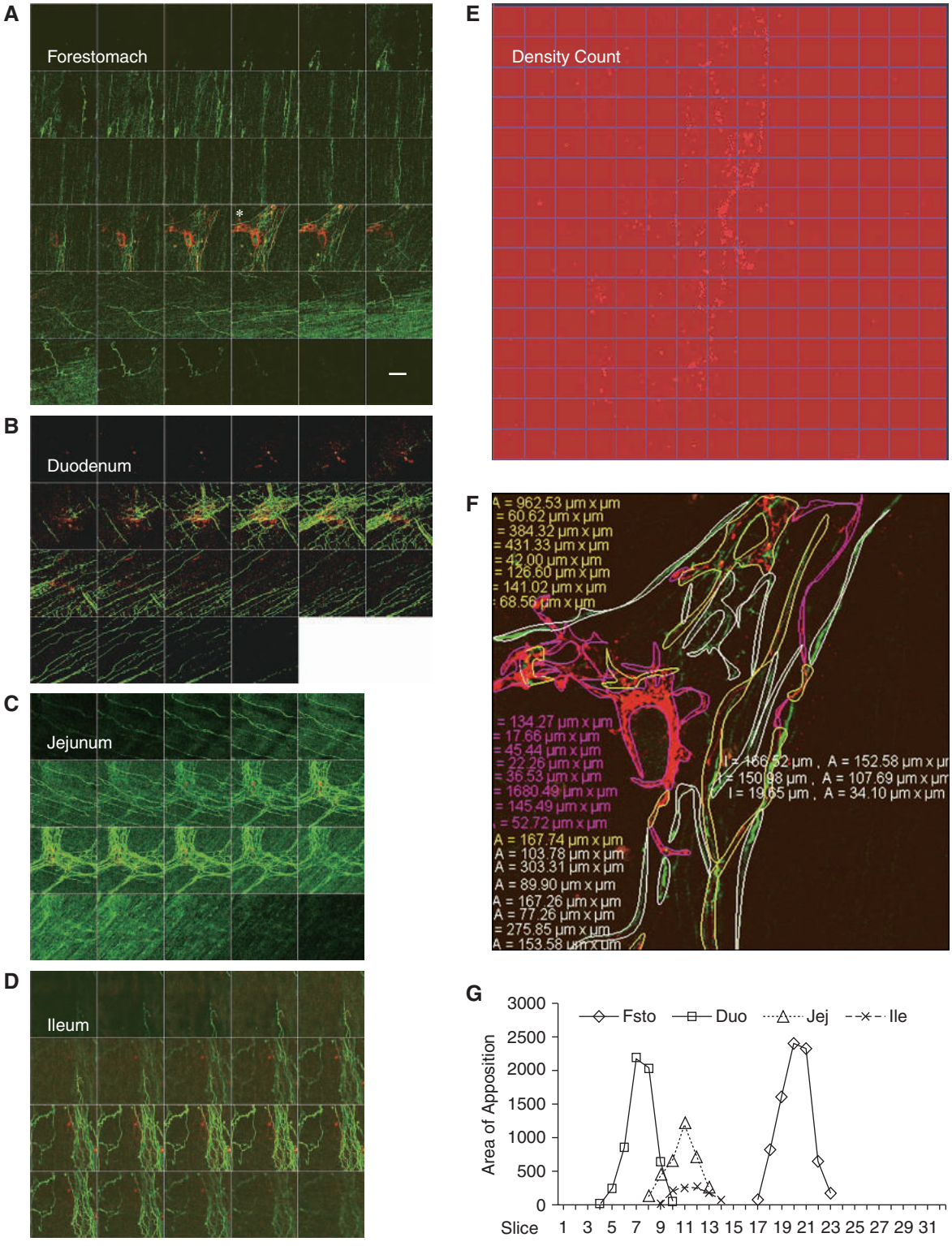

Fig. 1. Measurement of the density and area of the vagal and sympathetic efferent fibers in the myenteric plexus of the forestomach and small intestine. Panels A-D show the sequential optical sections of the vagal (red) and sympathetic (green) efferents in the forestomach and small intestine. Panel E (the same one as in Fig. 5D) shows the counts of intersection points crossed by the fibers with 16 × 16 grid lines (each with 230.3 μm length). Panel F is from the same figure as the one marked with a white star in Panel A and it shows the areas of the vagal and sympathetic efferents distributed in the myenteric plexuses of the forestomach and small intestines were estimated by contouring the outer edges of the autonomic fibers. Panel G shows the area of apposition starts from the circular muscle (slice 1) to the longitudinal muscle side (slice 31). Duo: duodenum; Fsto: forestomach; Ile: ileum; Jej: jejunum. Scale bar: 60 μm for A-D.

for both autonomic efferents starts from slice 1 in the circular muscle, reaches its peak at the middle section, and steadily declines at longitudinal muscle side up to slice 31 for the forestomach and slice 18 for the small intestines with different peak densities.

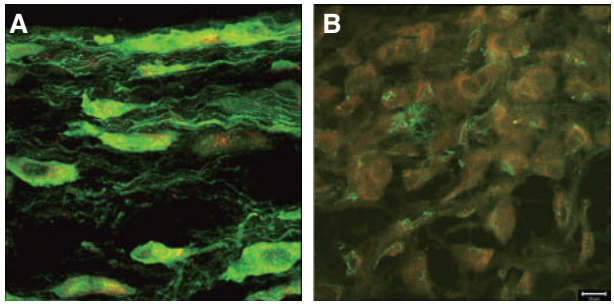

Fig. 2. Vagal (red) preganglionic and sympathetic (green) postganglionic tracing in the CG. Right CG (B) shows significantly denser vagal nerve endings than the left side (A). Scale bar: 20 μm.

Vagal and Sympathetic Efferent Innervations in the CG

The vagal nerve endings were densely distributed in the soma of the CG neurons (Fig. 2). Overall, the right CG received significantly more vagal innervations than the left CG (right: 76.82%, left: 14.51%; $t = 15.26$, n = 57, df = 112, $P < 0.01$). The MetaMorph analysis (Imaging Analysis System: MetaMorph v 4.5) shows that the mean area of the vagal preganglionic terminals that contact neurons of the CG is 45.67% of the overall area of the CG on both sides.

Vagal and Sympathetic Efferent Innervations in the Myenteric Plexus

Within the GI tract, the vagal efferent fibers are distributed within the connectives and ganglia of the myenteric plexus, and, upon entering a ganglion, produce different types of nerve endings containing dense terminal-like varicosities. Throughout the forestomach, duodenum, jejunum and ileum, sympathetic axons are much more

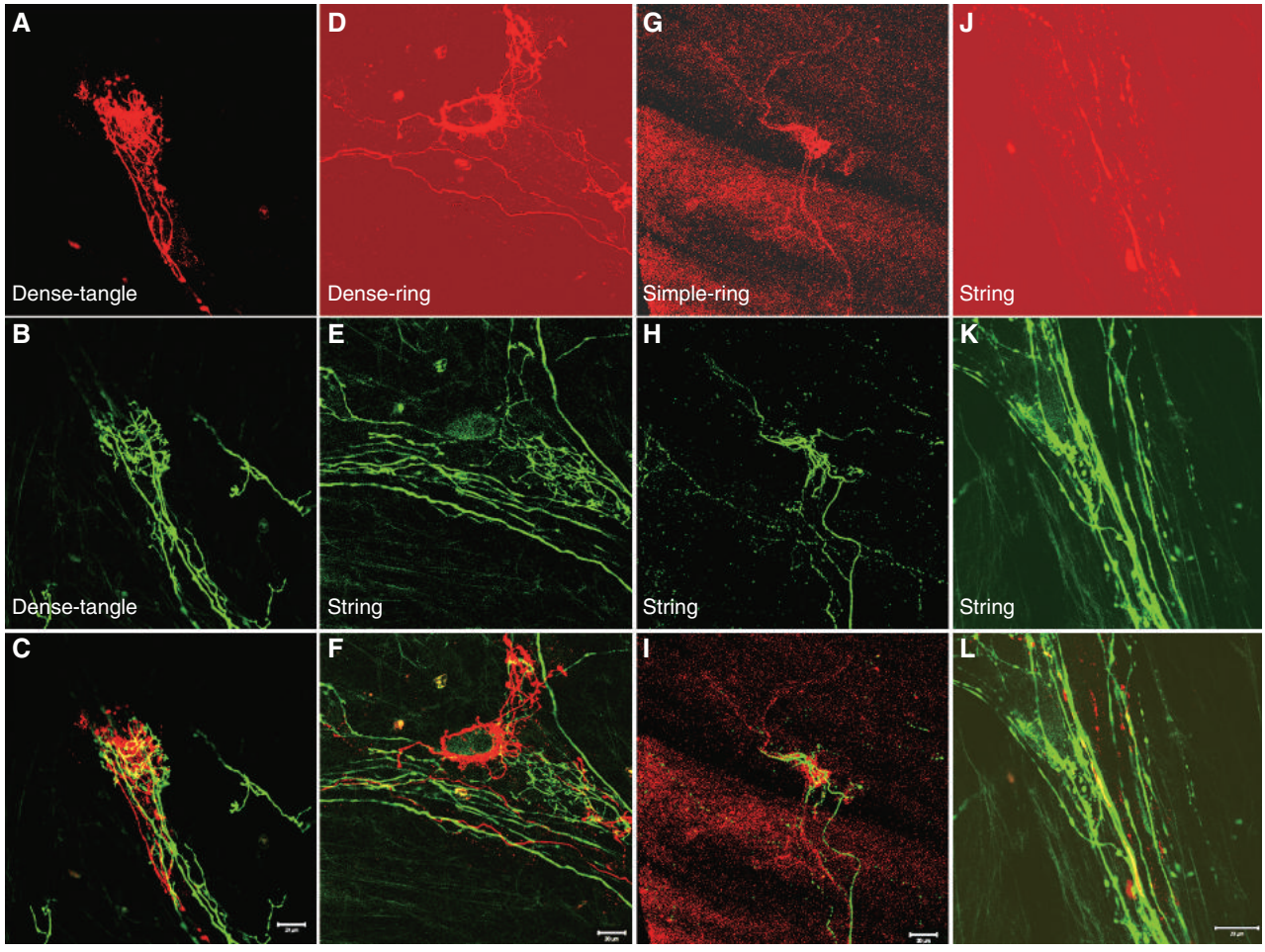

Fig. 3. Innervation types of vagal (red) and sympathetic (green) efferents in the myenteric plexus of the forestomach. Panels of the first row are for vagal efferents, the second for the sympathetic efferents, and the third for merged images o f both labeling. Scale bar: 20 μm.

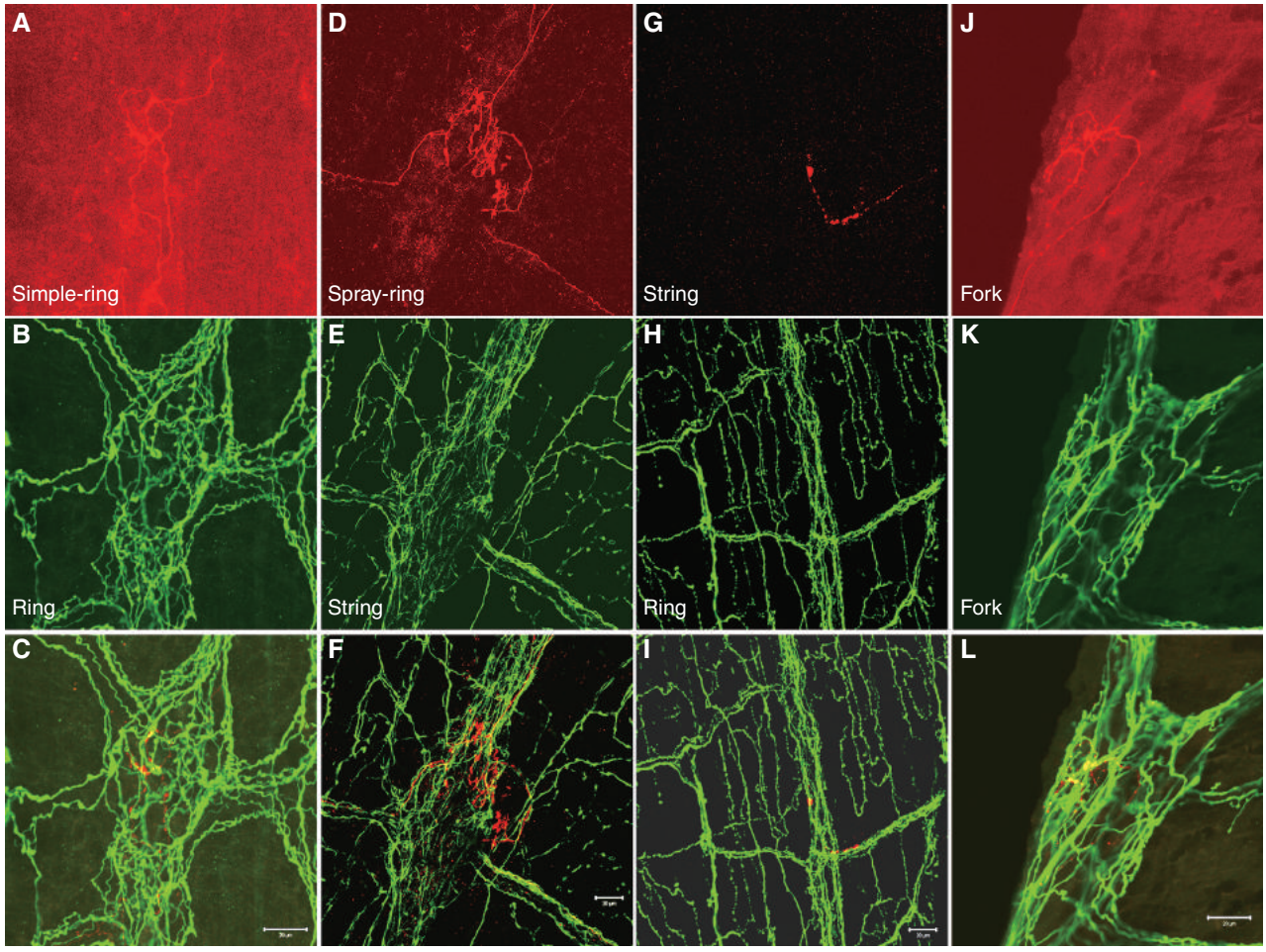

Fig. 4. Innervation types of vagal (red) and sympathetic (green) efferents in the myenteric plexus of the duodenum. Panels of the first row are for vagal efferents, the second for the sympathetic efferents, and the third for merged images of both labeling. Scale bar: 20 μm.

densely distributed in the myenteric plexus than the vagal efferents.

Autonomic efferent innervations in the forestomach. The paths of many Dextran-Texas Red-labeled vagal efferent axons and varicosities were found traveling either through or near the TH immunoreactive fibers. Four different types of vagal endings were found in the myenteric plexus of the forestomach: (1) "Dense-tangle type vagal efferents" that spray around one or more unstained neurons in the myenteric plexus and contain the dense-tangle type of sympathetic terminals run together and closely (Fig. 3, A-C); (2) "Dense-ring type vagal efferents" that circle around neuron in the myenteric plexus and include the string type of sympathetic fibers that contact only the outer edge of the ring (Fig. 3, D-F); (3) "Simple-ring type vagal efferents" that encircle the unstained neuron and consist of the string type of sympathetic fibers running through the circle (Fig. 3, G-I); (4) "String type vagal efferents" that have swollen varicosities and the string type of sympathetic fibers that run in close apposition with the vagal efferents (Fig. 3, J-L). Generally, vagal efferents in the forestomach run in apposition with the sympathetic fibers.

Autonomic efferent innervations in the duodenum. The labeled vagal and sympathetic axons are numerous in the myenteric plexus of the duodenum with four different types of terminal organization: (1) "Simple-ring type vagal efferents" are found in the myenteric plexus and the ring type of sympathetic terminals run closely together (Fig. 4, A-C); (2) "Spray-ring type vagal efferents" formulate dense rings with spray processings within it and the string type sympathetic fibers run only partly together with them (Fig. 4, D-F); (3) "String type vagal efferents" that run through the myenteric plexus and the ring type sympathetic fibers run together (Fig. 4, G-I); (4) "Fork type vagal efferents" with large swollen varicosities that partly circle the unstained neuron and the fork type sympathetic fibers run in close apposition with them (Fig. 4, J-L).

Autonomic efferent innervations in the jejunum. The vagal fibers labeled in the myenteric plexus of

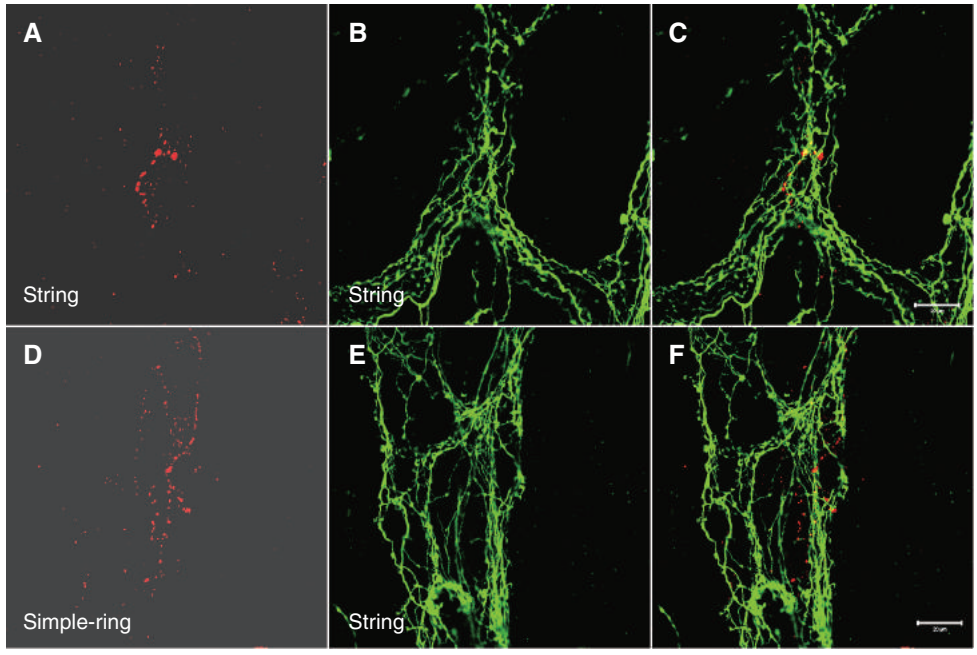

Fig. 5. Innervation types of vagal (red) and sympathetic (green) efferents in the myenteric plexus of the jejunum. Panels of the first column are for vagal efferents, the second for the sympathetic efferents, and the third for merged images of both labeling. Scale bar: 20 μm.

the jejunum are less dense than those found in the forestomach and duodenum, whereas the sympathetic axons in the jejunum are as numerous as those found in the duodenum. Only two different types of vagal terminal organization were found in the jejunum: (1) "String type vagal efferents" that contain several large varicosities distributed along the fiber and the string type sympathetic terminals that run closely with them (Fig. 5, A-C). (2) "Simple-ring type vagal efferents" that encircle the unstained neuron of the myenteric plexus and the string type sympathetic fibers run only partly together with them (Fig. 5, D-F).

Autonomic efferent innervations in the ileum. Vagal and sympathetic fibers labeled in the myenteric plexus of the ileum is less dense than those found in the forestomach, duodenum and jejunum, and three types of vagal terminal organization were found in the ileum: (1) "Simple-ring type vagal efferents" that encircle the unstained neuron and run independently from the fork type sympathetic fibers (Fig. 6, A-C); (2) "String type vagal efferents" that contain small varicosities and run together with the string type sympathetic fibers (Fig. 6, D-F); (3) "String-dot type vgal efferents" that contain small varicosities and run together with many string-dot varicosities of sympathetic fibers (Fig. 6, G-I).

Density of Autonomic Efferent Fibers in the Brightest Sections of Forestomach and Small Intestine

It is obvious that sympathetic fibers labeled are more numerous than vagal efferents in the myenteric plexus (Fig. 7). A two by four two-way (two autonomic efferents distributed in four different GI tract) ANOVA revealed significant ($P < 0.01$) main effects (for vagus and sympathetic: $F_{(3, 40)} = 6.52, 53.89, 34.47$; for four gut segments: $F_{(1, 40)} = 131.21, 1853.33, 705.19$) and interactions ($F_{(3, 40)} = 10.08, 127.49, 44.83$). The data also show that the ratios of the sympathetic fibers to vagal efferents under different objective lens (20x, 40x, 63x) for different tissues observed are: forestomach, 2:1, 2:1, 3:1; duodenum, 7:1, 7:1, 10:1; jejunum, 20:1, 14:1, 12:1; ileum, 8:1, 10:1, 7:1.

Posteriori comparisons (least significant difference, LSD test) indicate that the number of the sympathetic fibers is more abundant in the forestomach and increases significantly from duodenum to jejunum. However, the number of the sympathetic fibers in the ileum drops significantly. As for the vagal efferents, the number drops continuously from the forestomach to the ileum (Fig. 7). In the vagal efferents (the three bottom lines), the fiber density declines from forestomach to ileum; whereas in the sympathetic postganglionic fibers (three top lines), the density ascends from forestomach to duodenum and descends from duodenum to ileum. Overall, the sympathetic efferents are much denser than those of the vagal efferents, the duodenum and jejunum are much denser than those of the forestomach and ileum, and different powers of objective lens result in the same conclusion.

As shown in Fig. 8, under objective lens 40x (n = 6), area percentages of the vagal preganglionic only *vs*. sympathetic postganglionic efferents only *vs*. their

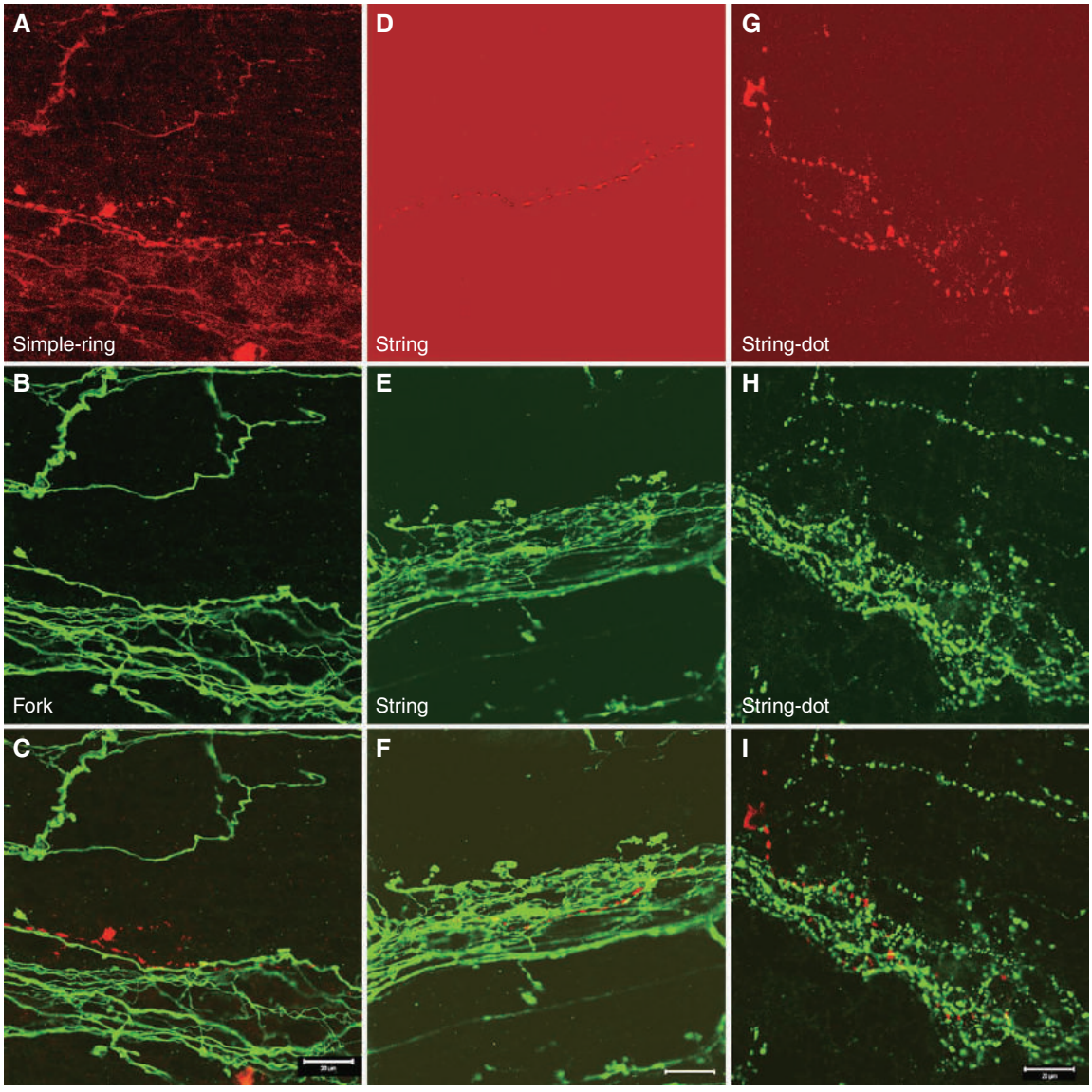

Fig. 6. Innervation types of vagal (red) and sympathetic (green) efferents in the myenteric plexus of the ileum. Panels of the first row are for vagal efferents, the second for the sympathetic efferents, and the third for merged images of both labeling. Scale bar: 20 μm.

in-apposition area distributed in the myenteric plexus of the forestomach and small intestines are: forestomach, 10.47%, 50.55%, 38.99%; duodenum, 1.67%, 89.90%, 8.43%; jejunum, 1.28%, 83.87%, 14.85%; ileum, 4.13%, 79.11%, 16.77%. Under objective lens 63x (n = 6), area percentages of the vagal preganglionic only *vs*. sympathetic postganglionic efferents only *vs*. their in-apposition area distributed in the myenteric plexus of the forestomach and small intestines are: forestomach, 0.79%, 96.28%, 2.93%; duodenum, 0.61%, 95.58%, 3.81%; jejunum, 1.06%, 87.99%, 10.94%; ileum, 3.25%, 73.07%, 23.68% (Fig. 8B).

A three by four two-way ANOVA (two autonomic efferents and their in-apposition areas--S, V, A--distributed in four different gut tissues) revealed significant ($P < 0.01$) main effects (for SVA: $F_{(2, 60)} = 30.07, 97.61$, $P < 0.01$; for four gut tissues: $F_{(3, 60)} = 10.96, 18.12$, $P < 0.01$) and interactions ($F_{(6, 60)} = 10.84, 17.78$) in four different areas measured with different objective powers (40x, 63x). With the posteriori comparisons (LSD), we found that the sympathetic efferents constitute a larger area than those of the vagus and areas in-apposition. On the other hand, the duodenum has larger area than those of the other gut tissues. Overall, the areas of the sympathetic efferents are much larger than those of the area in-apposition and the vagal efferents and the areas measured in the duodenum are significantly larger than those measured in other three different gut tissues. Furthermore, two different powers of objective lens result in the same conclusion.

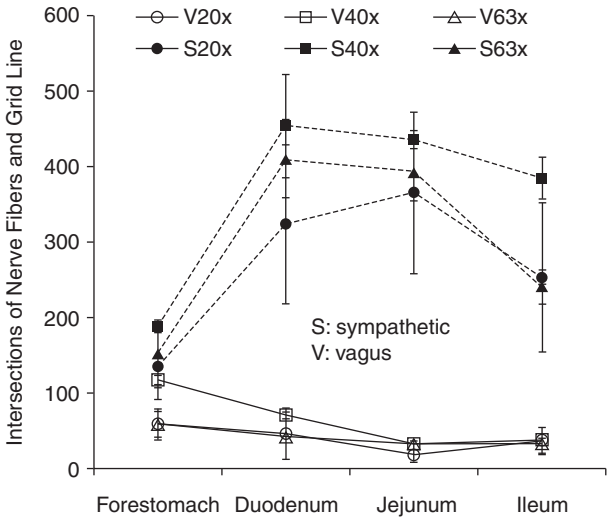

Fig. 7. Density count of vagal and sympathetic fibers in the myenteric plexus of the forestomach and small intestine. Images of the autonomic tracing (n = 6 for each group) were taken with three different objective lens, 20x, 40x, and 63x. The number of intersection points counted by the fibers crossing 16 × 16 square grid lines was used as the index of the density of the autonomic fibers. The fiber densities of vagal efferents (three bottom lines) decline from forestomach to ileum, whereas those of the sympathetic postganglionics (three top lines) ascend from forestomach to duodenum and descend from duodenum to ileum. V: vagal area; S: sympathetic area; A: both autonomic efferents.

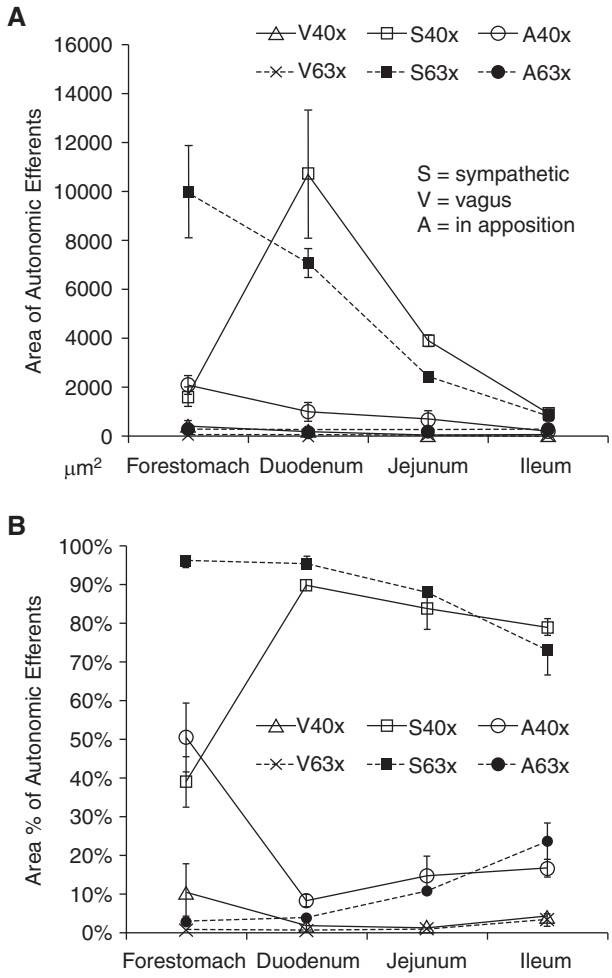

Fig. 8. Area and percentage comparison of the vagal and sympathetic efferents distributed in the myenteric plexuses of the forestomach and small intestines. Three different objective lens, 20x, 40x, and 63x were used for the measurement and comparison.

Vagal and Sympathetic Efferent Fibers Run Together with the SMA and Its Branches

Almost all of the vagal efferent fascicles as well as the bundles of sympathetic postganglionic fibers are enclosed within the same nerve bundles, ran together along the parent SMA (Fig. 9, A-D) and followed the smaller arterial branches to reach the intestine (Fig. 9, E-G). Each artery branch of the SMA has one pair of nerve bundles formed by the vagal and sympathetic efferents running in parallel with and distributed on the opposite side of the artery (Fig. 9, E-G). The bundles of sympathetic postganglionic fibers densely spread out to innervate the surface of the arterial branches (Fig. 10). The sympathetic fibers are the majority and the vagal efferents consisting of significantly fewer nerve bundles that run either on the parent SMA or its arterial branches. It is important to note that the vagal efferents rarely run alone on the surface of the blood vessel (Fig. 10A). As measured for the GI tract, the area percentages for the sympathetic efferents, vagal efferents and both autonomic efferents running in-apposition in the parent SMA are respectively measured with 63x power as 56.06%, 0.08%, and 43.86% (paired two-tailed, t = -6.30, df = 13, P < 0.01); and for the finer arterial branches as 93.08%, 0.04%, and 6.88% (paired two-tailed, t = -5.83, df = 12, P < 0.01) with significant difference.

Discussion

A profile that shows how the vagal preganglionic and sympathetic postganglionic efferents are arranged along the sub-branches of the SMA and in the abdominal viscera may offer us some insight for the infection routes of the Parkinson's disease. We double labeled the vagal preganglionic and the sympathetic postganglionic fibers in the CG, SMA and its finer branches, and the abdominal GI tract of the rat. In agree-ment with an earlier report (2), neurons in the CGs are innervated by the vagal preganglionics. Furthermore, the right CG receives denser vagal efferent innervations than does the left side. The functional meaning of this lateralized innervation is to be examined.

In consistent with the earlier report, the sympa-

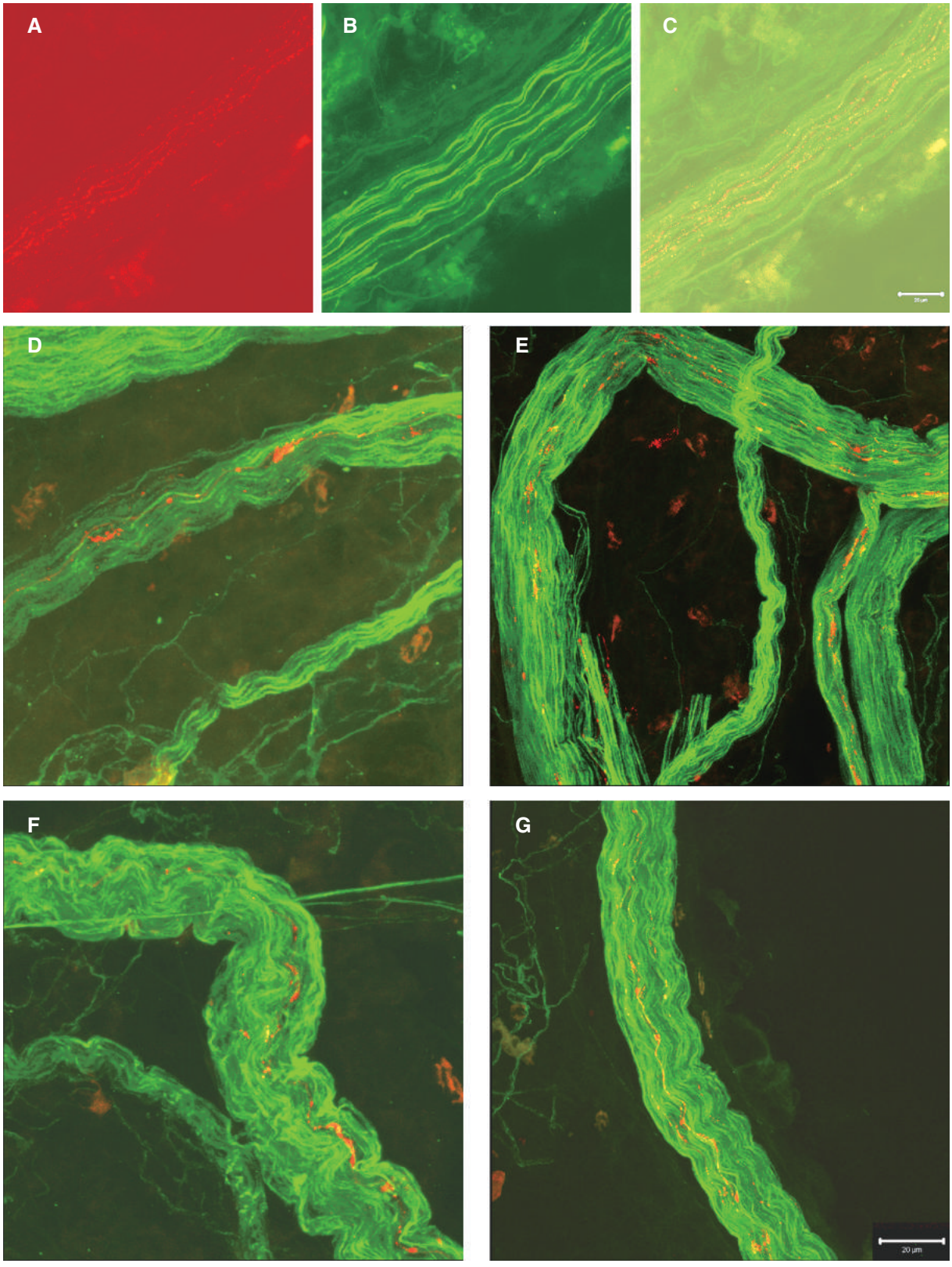

Fig. 9. Vagal (red) and sympathetic (green) efferents ran together within the same nerve bundle and along the parent vessels and smaller branches of the SMA. Images from paneld A to D show the efferents running along the parent SMA. The fluorescence of the vagal efferents was visible but too weak to be scanned well. Panel C is a merge of A and B. Panels E-G show the efferents running along the smaller branches of the SMA. The vagal efferents give swollen varicosities in apposition with the sympatheric fibers. Scale bar: 20 µm (A-G).

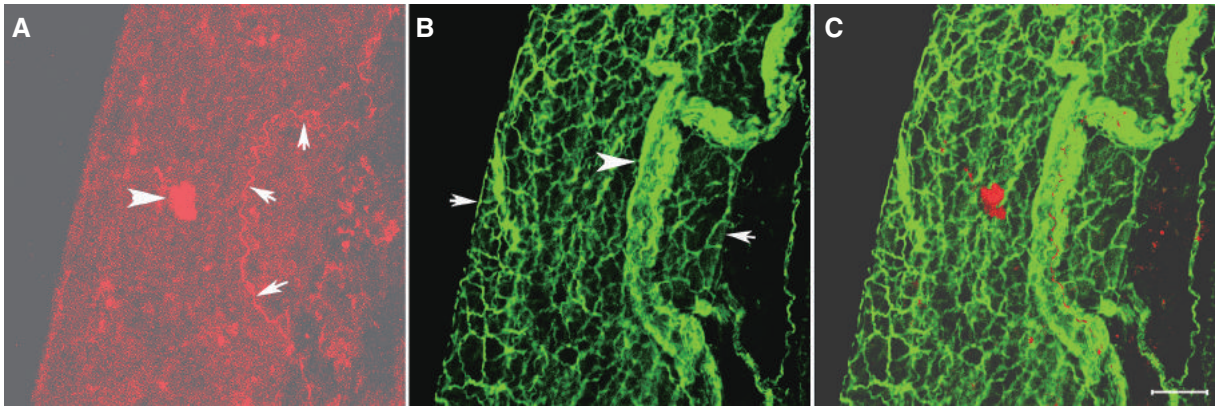

Fig. 10. Vagal and sympathetic endings circle around the smaller branching vessel of the SMA. Panel A shows the vagal preganglionic fiber (arrows) that rarely running on the surface of the small blood vessel with presumably direct contact. The arrow head indicates an artifact. Panel B shows the edges of the blood vessel as indicated by two arrows and the nerve bundle by the arrow head. Scale bar: 60 μm.

thetic efferent fibers together with the vagal efferents are enclosed within the same nerve bundles running along the SMA and its finer branches on the way to innervate the GI tract (23). Inventories of the vagal and sympathetic efferents include various types/shapes of nerve endings with in-apposition varicosities are distributed in the forestomach, duodenum, jejunum, and ileum. With this inventory, we provide the basis to consider the infection route of the Parkinson's disease and to re-think the neural control mechanism for the "fight-or-flight" emotional response.

Strong Sympathetic and Weak Vagal Tracing: Methodological Consideration

It has been shown that the stomach is heavily innervated by the vagal efferents in the rat (1, 8). Here we showed the sympathetic efferents were labeled much stronger than the vagal efferents in the forestomach and small intestines. Methodologically, the sympathetics can be stained completely with the immunohistochemistry for TH. However, the vagal preganglionics are always labeled partially and incompletely because the tracer injections into the dmnX may damage or eliminate some neurons (17). Thus, the dual labeling strategy we used here would almost certainly exaggerate the relative disparity in numbers or proportions between sympathetic and parasympathetic efferents. Nevertheless, the drop of labeling from the forestomach and duodenum to the caudal intestine is consistent with our earlier tracing pattern for the vagal afferents (22). It is known that the abdominal vagal trunks and nerves contain catecholaminergic fibers coming from neurons in the dorsal motor nucleus of the vagus with the number of 215 (25) or 335 (19) and nodose ganglion with the number of 47 (25). Furthermore, these small amounts of fibers are primarily dopaminergic and of parasympathetic origin and only an extremely small number of them are mostly noradrenergic in nature and arise from postganglionic sympathetic neurons (25). Since our current tracing method may contain some bias to cause an underestimate for the vagal efferents and the small amount of vagal dopaminergic fibers could also be counted as sympathetic ones, a dual labeling with adrenergic stain for the sympathetics and cholinergic stain for the vagus may offer a better way to confirm our current conclusion that the sympathetics in the blood vessels and myenteric plexus are more prominent than the vagal efferents (Figs. 7 and 8).

Inventory of Vagal Preganglionic and Sympathetic Postganglionic Efferent Nerve Endings

Earlier sympathetic and vagal traicings in the GI tract focused mainly on the detailed individual terminal varicosities that contact the dendritic and somatic architecture of counterstained neurons in the myenteric plexus. In general, the morphological descriptions of current sympathetic postganglionic and vagal preganglionic terminal endings in the GI tract are in agreement with earlier reports that did not attempt to make the inventory of the shapes of the autonomic nerve endings (13, 14, 20). Since we did not work further on the neurochemistry of the sympathetic and vagal efferents and the interaction or in-apposition areas at the terminal endings were our observation focus, neutral descriptive terms were chosen in this study for the different classes of efferent terminals. These arbitrarily classified types of the sympathetic and vagal efferents could be summarized as two different types: 1) the "loose" type, including the simple-ring and string type, that has string line(s) or simple ring to form simple contact with the myenteric neurons, and 2) the "dense" type, including the dense-tangle and dense-ring type,

that has dense and complex ring to tangle with each other to wrap up the myenteric neurons.

We delineated several different types of autonomic nerve endings innervating the myenteric plexus of the forestomach and small intestines. With regard to the vagal nerve endings, ring type and string type are typical types (Figs. 3-6). However, the special types are dense-tangle type in the forestomach (Fig. 3), fork type in the duodenum (Fig. 4) and string-dot type in the ileum (Fig. 6), respectively. As to the sympathetic fibers, string type is the typical type (Figs. 3-6). While, the special types are dense-tangle type in the forestomach (Fig. 3), fork type in the duodenum (Fig. 4) and ileum, and string-dot type in the ileum (Fig. 6).

Furthermore, vagal and sympathetic efferents are enclosed within the same nerve bundles and run in parallel with the SMA and their small branches (Fig. 9). Almost all of the autonomic fibers that run together have swollen varicosities in close apposition with each other. This in-apposition innervation pattern may indicate facilitated chemical interactions on the same tissue (8). The abundant combination of these different types of autonomic nerve endings might indicate the versatile interaction of the vagal efferens and sympathetic postganglionic fibers communicating with the myenteric neurons.

Dense Contacts of Vagal and Sympathetic Postganglionic Efferent Nerve Endings

Braak and his colleagues (3, 6) have proposed a novel explanation that Parkinson's disease starts in the enteric nervous system and pathogens spread to the central nervous system *via* vagal preganglionic innervation of the gut. In addition, the postganglionic sympathetic neurons located in the CG that influences the input into the enteric nervous system and a large proportion of neurons develop the same form of Parkinson's disease associated lesions (4).

In the present study, we traced the vagal preganglionics and sympathetic postganglionic nerves and endings in the CG and the myenteric plexus of the gut. Both autonomic efferent components run together and densely form the in-apposition varicosities. This structural alignment is consistent with the fact that neurons in the CG also develop Parkinson's disease associated lesions and the vagal preganglionic in the stomach is the most likely starting point for pathological insult (9). Furthermore, both the vagal and sympathetic efferent components also have dense in-apposition varicosities in the blood vessels and myenteric plexuses examined in the gut. This pea- and-carrot type of innervation pattern highly increases the infection possibility from the vagal preganglionic components to the sympathetic postganglionic ones or *vice versa*.

Predominant Sympathetic Contacts to the Myenteric Plexus and in the Blood Vessels

The stomach is "heavily" innervated by the vagal preganglionics (1, 8). Here we show that the number of sympathetic postganglionic fibers overwhelm that of the vagal preganglionic fibers in the CG (Fig. 2), the myenteric plexus in the forestomach, duodenum, jejunum and ileum (Figs. 3-8), and the surface of the blood vessels (Figs. 9 and 10). Corresponding to our earlier vagal tracing (23), each artery branch of the SMA usually has one pair of nerve bundles formed by the vagal and sympathetic efferents run in parallel with and distributed on the opposite side of the artery (Fig. 9, E-G). Moreover, the bundles of sympathetic postganglionic fibers densely spread out to innervate the surface of the arterial branches (Fig. 10B). Briefly, the sympathetic fibers are the majority and the vagal effernts rarely present on the surface of the finer blood vessels (Fig. 10A). The weakly labeled vagal efferents on the surface of the vasculatures might have been easily neglected in the past and should receive further examination for their existence and function.

Based on the fact that the sympathetic limb can rapidly re-allocate the blood volume from the abdominal cavity to the four limbs that must be ready for "fight-or-flight" response, we may presume that the super-predominant synaptic contacts of the sympathetic postganglionic components in the blood vessels and myenteric plexuses layout the basic neural structure to regulate the rapid "fight-or-flight" response. In addition to the chemical regulation, the rapid onset and slow recovery of the emotional response could be illustrated by these autonomic innervation patterns.

There is always one pair of nerve bundles running along the second-order of the SMA and down to the finer bundles. The GI tract is innervated by intrinsic enteric neurons and by extrinsic projections, including sympathetic projections (celiac, superior and inferior mesenteric ganglia by the mesenteric and splanchnic nerves) and parasympathetic projections as well as visceral afferents (21). Since both vagal preganglionic and sympathetic postganglionic fibers are enclosed within the same nerve bundles travelling along the branches of the SMA, it is quite possible that all of the neural components that innervate the gut may also take the same routes to their targets to implement their functions.

Together with the wide contacts of vagal efferent fibers to neurons in the prevertebral ganglia (2), the tight contacts of the vagal preganglionic and sympathetic postganglionic motor fibers along the mesenteric arteries and in the myenteric plexus offer three possible infection routes or sites for the Parkinson's disease to be further examined: [1] vagal preganglionic

elements and the postganglionic neurons in the prevertebral ganglia, [2] vagal preganglionic nerve endings and the postganglionic elements coming from the prevertebral ganglia, and [3] the two bundles of fibers running along the sub-branches of the superior mesentery artery.

Acknowledgments

This study was sponsored by National Chung Cheng University (Z100, Z31, 3140306-01, 085-00002-01), Ministry of Education (99CE096, 090-00033-01), Ministry of Science and Technology (MOST 104-2410-H-194-033), and National Science Council, Taiwan, Republic of China (NSC42114F, NSC91-2413-H-194-017, NSC90-2413-H-194-023, NSC88-2413-H-194-014, NSC87-2413-H-194-012, NSC86-2418-H-194-003-T), Academic Foundation and Advanced Institute of Manufacturing with High-tech Innovations of Chung Cheng University for FBW, as well as by Graduate Scholarship of the Department of Psychology, National Chung Cheng University for SJT. We thank Drs. Sigmund Hsiao and Terry L. Powley for their comments, Drs. Terry L. Powley and Robert J. Phillips for their technical demonstration and advice on the TH immunohistochemistry, and Dr. Yi-Han Liao for her experimental support. This report was presented as an abstract in the annual meeting of The Taiwanese Psychological Association (Oct, 2011).

References

1. Berthoud, H.R., Carlson, N.R. and Powley, T.L. Topography of efferent vagal innervation of the rat gastrointestinal tract. *Am. J. Physiol.* 260: R200-R207, 1991.
2. Berthoud, H.R. and Powley, T.L. Interaction between parasympathetic and sympathetic nerves in prevertebral ganglia: morphological evidence for vagal efferent innervation of ganglion cells in the rat. *Microsc. Res. Tech.* 35: 80-86, 1996.
3. Braak, H., Rub, U., Gai, W.P. and Del Tredici, K. Idiopathic Parkinson's disease: possible routes by which vulnerable neuronal types may be subject to neuroinvasion by an unknown pathogen. *J. Neural. Transm.* 110: 517-536, 2003.
4. Braak, H., Sastre, M., Bohl, J.R., de Vos, R.A. and Del Tredici, K. Parkinson's disease: lesions in dorsal horn layer I, involvement of parasympathetic and sympathetic pre- and postganglionic neurons. *Acta Neuropathol.* 113: 421-429, 2007.
5. Cannon, W.B. *The Wisdom of the Body,* Norton, New York, 1932.
6. Del Tredici, K., Rub, U., De Vos, R.A., Bohl, J.R. and Braak, H. Where does Parkinson disease pathology begin in the brain? *J. Neuropathol. Exp. Neurol.* 61: 413-426, 2002.
7. Furness, J.B. and Costa, M. The adrenergic innervation of the gastrointestinal tract. *Ergeb. Physiol.* 69: 2-51, 1974.
8. Holst, M.-C., Kelly, J.B. and Powley, T.L. Vagal preganglionic projections to the enteric nervous system characterized with PHA-L. *J. Comp. Neurol.* 381: 81-100, 1997.
9. Hawkes, C.H., Del Tredici, K. and Braak, H. Parkinson's disease: a dual-hit hypothesis. *Neuropathol. Appl. Neurobiol.* 33: 599-614, 2007.
10. Li. J.Y., Jensen, P.H. and Dahlstrom, A. Differential localization of alpha-, beta- and gamma-synucleins in the rat CNS. *Neuroscience* 113: 463-478, 2002.
11. Mawe, G.M., Schemann, M., Wood, J.D. and Gershon, M.D. Immunocytochemical analysis of potential neurotransmitters present in the myenteric plexus and muscular layers of the corpus of the guinea pig stomach. *Anat. Rec.* 224: 431-442, 1989.
12. Olsson, C., Costa, M. and Brookes, S.J. Neurochemical characterization of extrinsic innervation of the guinea pig rectum. *J. Comp. Neurol.* 470: 357-371, 2004.
13. Phillips, R.J., Rhodes, B.S. and Powley, T.L. Effects of age on sympathetic innervation of the myenteric plexus and gastrointestinal smooth muscle of Fischer 344 rats. *Anat. Embryol.* 211: 673-683, 2006.
14. Phillips, R.J., Walter, G.C., Wilder, S.L., Baronowsky, E.A. and Powley, T.L. Alpha-synuclein immunopositive myenteric neurons and vagal preganglionic terminals: autonomic pathway implicated in Parkinson's disease? *Neuroscience* 153: 733-750, 2008.
15. Phillips, R.J. and Powley, T.L. Tension and stretch receptors in gastrointestinal smooth muscle: reevaluating vagal mechanoreceptor electrophysiology. *Brit. Res. Rev.* 34: 1-26, 2000.
16. Powley, T.L. and Phillips, R.J. Musings on the wanderer: what's new in our understanding of vago-vagal reflexes? I. Morphology and topography of vagal afferents innervating the GI tract. *Am. J. Physiol. Gastrointest. Liver Physiol.* 283: G1217-G1225, 2002.
17. Powley, T.L. and Phillips, R.J. Advances in neural tracing of vagal afferent nerves and terminals. In: *Advances in vagal afferent neurobiology*, edited by Undem, B.J. and Weinreich, D. Boca Raton, FL, USA: CRC Press, Taylor & Francis Group, LLC, 2005, pp.123-145.
18. Powley, T.L. and Phillips, R.J. Vagal intramuscular array afferents form complexes with interstitial cells of Cajal in gastrointestinal smooth muscle: analogues of muscle spindle organs? *Neuroscience* 186: 188-200, 2011.
19. Tayo, E.K. and Williams, R.G. Catecholaminergic parasympathetic efferents within the dorsal motor nucleus of the vagus in the rat: a quantitative analysis. *Neurosci. Lett.* 90: 1-5, 1988.
20. Walter, G.C., Phillips, R.J., Baronowsky, E.A. and Powley, T.L. Versatile, high-resolution anterograde labeling of vagal efferent projections with dextran amines. *J. Neurosci. Methods* 178: 1-9, 2009.
21. Wang, F.B., Holst, M.C. and Powley, T.L. The ratio of pre- to postganglionic neurons and related issues in the autonomic nervous system. *Brain Res. Rev.* 21: 93-115, 1995.
22. Wang, F.B. and Powley, T.L. Topographic inventories of vagal afferents in gastrointestinal muscle. *J. Comp. Neurol.* 421: 302-324, 2000.
23. Wang, F.B. and Powley, T.L. Vagal innervation of intestines: afferent pathways mapped with new en bloc horseradish peroxidase adaptation. *Cell Tissue Res.* 329: 221-230, 2007.
24. Wang, F.B., Young, Y.K. and Kao, C.K. Abdominal vagal afferent pathways and their distributions of intraganglionic laminar endings in the rat duodenum. *J. Comp. Neurol.* 520: 1098-1113, 2012.
25. Yang, M., Zhao, X. and Miselis, R.R. The origin of catecholaminergic nerve fibers in the subdiaphragmaticvagus nerve of rat. *J. Auton. Nerv. Syst.* 76: 108-117, 1999.